Space Launch System Base Heating Test: Tunable Diode Laser Absorption Spectroscopy

Ron Parker[1]
Zak Carr[2]
Mathew MacLean[3]
Aaron Dufrene[4]
CUBRC Inc., Aerosciences Division, Buffalo, NY, 14225

Manish Mehta[5]
NASA Marshall Space Flight Center MSFC, AL 35812

This paper describes the Tunable Diode Laser Absorption Spectroscopy (TDLAS) measurement of several water transitions that were interrogated during a hot-fire testing of the Space Launch Systems (SLS) sub-scale vehicle installed in LENS II. The temperature of the recirculating gas flow over the base plate was found to increase with altitude and is consistent with CFD results. It was also observed that the gas above the base plate has significant velocity along the optical path of the sensor at the higher altitudes. The line-by-line analysis of the H_2O absorption features must include the effects of the Doppler shift phenomena particularly at high altitude. The TDLAS experimental measurements and the analysis procedure which incorporates the velocity dependent flow will be described.

I. Introduction

CUBRC is supporting testing of a sub-scale hot-fire model for NASA's design of the Space Launch System (SLS) vehicle. The SLS vehicle is composed of four RS-25D LOX/LH2 rocket engines in the core stage and two 5-segment solid rocket motors for the booster stage. It is designed to take NASA beyond low-earth-orbit for the first time in over forty years using geometry and rocket motors that are significantly different than previously-flown systems. Convective base heating testing is one of a series of ground tests required to successfully develop this next generation rocket. Rocket motor plume interaction drives base heating and is extremely complex and difficult to simulate with modern computational fluid dynamic tools. Ground experiments of a 2% scale model operating near flight-scale pressures with flight-like propellant at duplicated flight conditions have been and continue to be tested in the LENS II shock tunnel. A picture of the model in the tunnel is shown in Fig. 1.

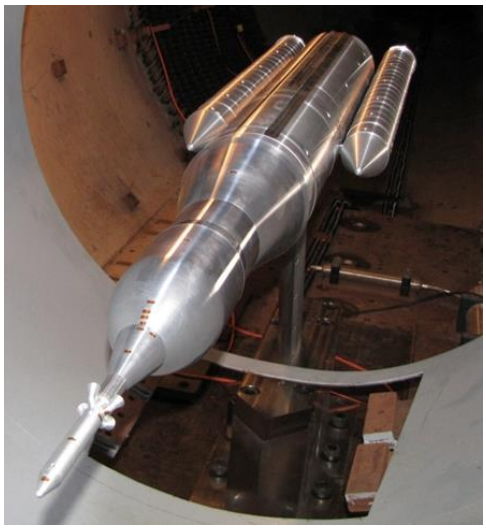

Figure 1 SLS Hot-Fire model installed in the LENS II facility.

These ATA-002 tests will help NASA MSFC in developing ascent plume induced thermal design environments for the SLS vehicle.

The primary goal of the ATA-002 test program is to define the base heating environment. Heat transfer measurement with fast-response thin-film heat transfer gauges or thermocouples is a common, well-understood diagnostic and represents the majority of the measurements in this program. Pressure and radiometer measurements are also made in the base region to help

[1] Senior Research Scientist; CUBRC Aero-sciences group, AIAA Senior Member
[2] Research Scientist; CUBRC Aero-sciences group, AIAA Member
[3] Senior Research Scientist; CUBRC Aero-sciences group, AIAA Senior Member
[4] Research Scientist; CUBRC Aero-sciences group, AIAA Member
[5] Research Scientist; NASA Marshall Space Flight Center AIAA Member

define the surface environments. Scaling 2%-model-scale heat transfer data to flight is complicated by the fact that gas temperature and composition is unknown. Typical aerothermal scaling is not difficult, because the tunnel freestream conditions are well defined, but plume interactions are poorly understood. This was a major source of uncertainty for previous Space Shuttle base heating studies [1, 2]. There were two approaches to determine gas temperature in previous testing. The first method relied on platinum-rhodium thin-wire resistance temperature detectors (RTDs) [3]. These are minimally-heated hot-wire probes that heat up when exposed to the rocket exhaust. Gas properties are unknown, so two different length wires and a complex analysis is required to reduce the temperature data. This measurement is intrusive and often had uncertainties of several hundred degrees Rankine. The second method utilized a heated base plate and high-temperature thin-film heat flux instruments [4]. As the wall temperature increases heat transfer decreases linearly to the gas recovery temperature. Therefore, from tests performed with the base plate heated to several different temperatures, gas temperature can be extrapolated. This method is nonintrusive, but has downsides including the need to perform several runs to obtain one gas temperature measurement, and the need to use high-temperature instrumentation which limits the instrumentation options. These measurements require a complex setup, and other parts of the model such as nozzle or central combustor can be inadvertently heated which may affect measured heat transfer. Also, as the wall is heated heat transfer goes down and the signal-to-noise ratio of the heat transfer measurements is reduced.

Both gas temperature measurement methods used in the Space Shuttle base heating studies are being used in the ATA-002 program in slightly altered forms. Instead of the thin-wire RTDs, thin-wire thermocouples of different diameters are being used. This change was made as a recommendation from engineers involved in the previous NASA base heating studies. Data reduction should be simpler and uncertainty should be lower. Also, a limited number of tests where the base plate is heated were performed, but the majority of runs were be done with highly-instrumented nozzles and base plate.

The importance of this base-gas temperature measurement, and the high uncertainty reported in previous programs motivated the development of an instrument that was based on tunable diode laser absorption spectroscopy (TDLAS) which shows promise as a more accurate, non-intrusive measurement of path-averaged base gas temperature.

The LENS II Facility and the sub-scale NASA SLS model

SLS base heating studies are being conducted in the LENS II shock and Ludwieg tunnel. Data from this test will assess peak convective heat flux design sensitivity concerns. Testing includes first-stage testing with all four core-stage engines and both solid rocket motors as well as second-stage tests post SRB separation with and without tunnel flow. LENS II is capable of operating over a Mach range of $2.7 \leq M_\infty \leq 9.25$ and pressure altitudes of sea-level $\leq H \leq 200$kft (Fig. 2). Testing was split up into two phases, with the first phase focused on developing the 2% scale hydrogen/oxygen engines and solid rocket motors [5]. After a successful sub-scale rocket motor development program, a 2% scale SLS model was fabricated and instrumented for the base-heating studies at a variety of Mach numbers and altitudes at duplicated flight conditions. Scaled freestream conditions are designed to match flight conditions exactly, as opposed to typical scaled Reynolds number testing. This is done to preserve the plume expansion and interaction region which has a first-order effect on base heating levels. Model boundary layer conditions do not match flight-scale, but analysis indicates boundary layer state and size

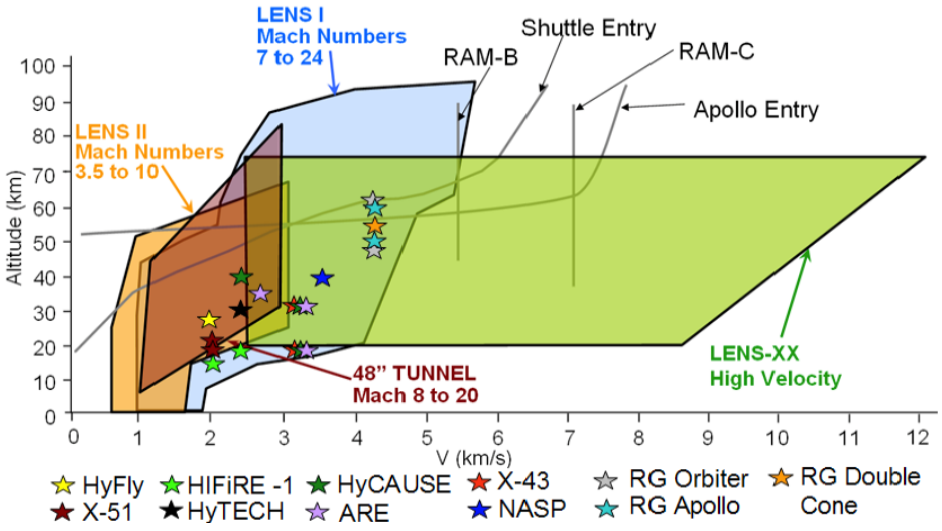

Figure 2. Velocity/Altitude Capabilities of the LENS Shock Tunnels and Expansion Tunnel

are not drivers in base heating levels.

Short-duration testing is critical to model and instrument reusability, so test time is long enough to obtain high-quality steady measurements, but short enough to ensure reusability of the hardware. A typical timing sequence is shown in Fig. 3, showing that the flow over the model starts just prior to, or coincident with, the ignition of the solid rocket motors. Compared to the core stage, the solid rocket motors take longer to start and become steady so the core-stage engine firing is delayed by 10-15ms. All engines are firing for a steady-state test time of ~50ms, at which point the core-stage engines shut down immediately, and solid rocket motors begin to slowly shut down. Tunnel test time is up to 300ms at lower velocity/lower Mach number conditions and as short as 20ms at high velocity/Mach number conditions, so repeatable and accurate timing of rocket motors and tunnel operation has been demonstrated and is critical to successful base heating studies.

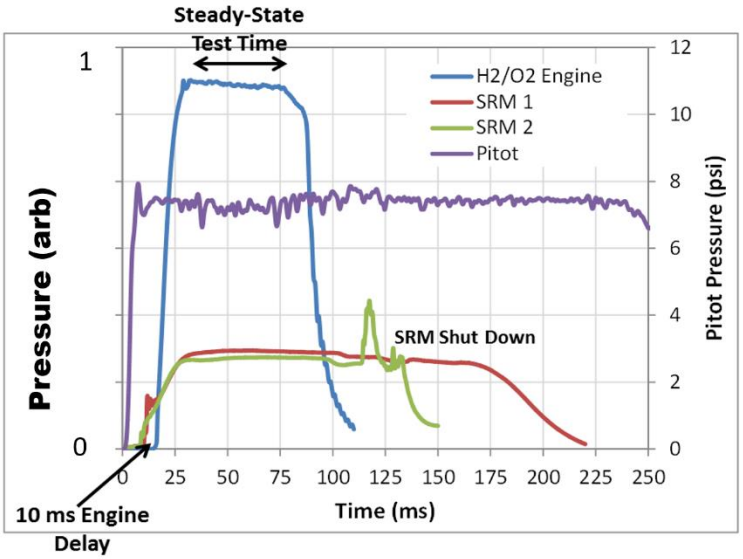

Figure 3. Typical timing sequence for 2%-scale SLS base heating hot-fire testing.

A photograph of all engines firing near full-scale pressures in a Mach 2.8 flow at approximately 70kft is shown in Fig. 4. The four hydrogen/oxygen engines are ported from a central combustor to minimize thrust/pressure mismatches and to simplify the model propulsion system. Gaseous hydrogen and oxygen are fed through flow-control venturis that set the O/F ratio to match the RS-25 engines, and constant pressure is maintained through long constant-diameter charge tubes. Gas flow is initiated by opening fast-response balanced poppet solenoid valves and the ignition source is an exposed wire glow plug. The central combustor reaches steady state engine pressure in less than 20ms from sending the valve triggering signal. Specific details of engine performance and development are reported in Ref. (6).

The solid rocket motors use an ammonium perchlorate/high-aluminum-loaded solid propellant grain that is analogous to the RSRM propellant. Thin cylindrical propellant castings are used to ensure even burning and achieve steady chamber pressures. The ignition source is a hydrogen/oxygen torch that adds less than 2% water to the combustion products, which is already dominated by water. Other ignition sources did not prove fast enough to get the solid rocket motors up to full, steady pressure within 30ms. Specific details of motor performance and development are reported in Ref. (7).

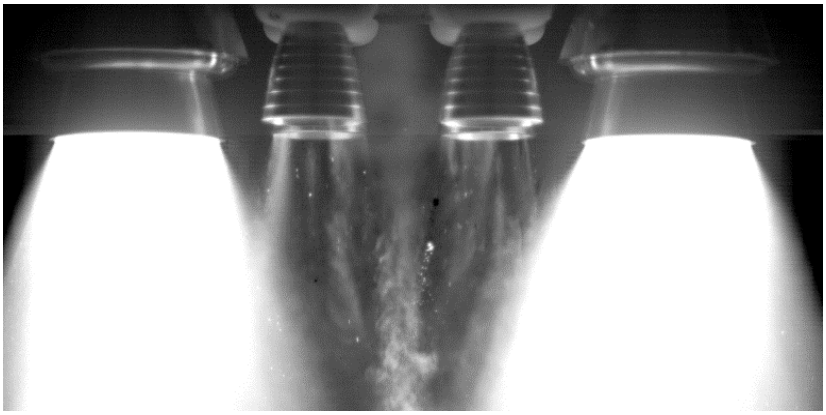

Figure 4. 2%-scale SLS hot-fire test at Mach 2.8, 70kft condition.

II. Instrumentation and Experimental Setup

A. TDLAS Instrument

Tunable Diode Laser Absorption Spectroscopy is an active non-intrusive technique which allows the experimenter to ascertain the properties of the target molecules which interact with the laser radiation. A beam of photons projected through the gas can result in specific absorption features that are measured as the beam is scanned in wavelength. Analysis of the exact shape of these absorption features results in a direct measurement of the molecules temperature, pressure, density and even velocity [8-10].

A Quantum Cascade Laser (QCL) from nano-plus technologies[11] that operates at 2713 nm was used to probe individual rotational-vibrational transitions of the H_2O molecule which is the major combustion by-product of the hot-fire model with its four H_2/O_2 rockets and two solid rocket motors. The QCL source is a high power diode laser with extremely narrow emission line width, much narrower by a factor of 100 or more, than the typical very narrow rotational-vibrational absorption feature of a diatomic or triatomic gas at low pressure for a high altitude trajectory during rocket ascension. These inexpensive diode laser sources have low power requirements, and an integrated thermo-electric cooler, similar to telecommunication diodes which are in common use. Optical fibers which transmit at 2700 nm are now common which allow simple coupling of the source and receive radiation to the hostile testing environment. A schematic representation, Fig. 5, shows the components required for the pitch-catch optical probe to measure the gas temperature above the base plate of the 2 percent SLS model shown in Fig. 1. The QCL source is mounted on an optical plate on top of the LENS II tunnel. The source radiation is coupled to a single mode optical fiber and fed through a vacuum fitting to an optical telescope mounted above the model base plate as represented in Fig. 5. A mirror is mounted below the base plate such that the source radiation reflects off the mirror and follows an almost identical optical path to a receive telescope that is mounted beside the source telescope. The laser radiation is captured by that telescope and fed to a multimode fiber that is likewise passed through the vacuum fitting to a detector. This optical setup was very robust and required only minor tweaking over 50+ measurements that were performed on the base plate for various altitudes and Mach numbers spanning the flight trajectory of the SLS vehicle during ascent into space.

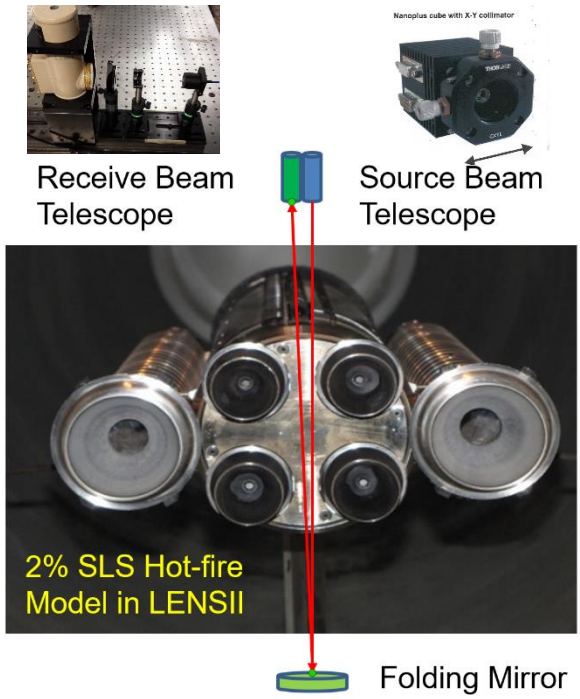

Figure 5. A schematic representation of the pitch/catch arrangement for the TDLAS experiment in LENS II.

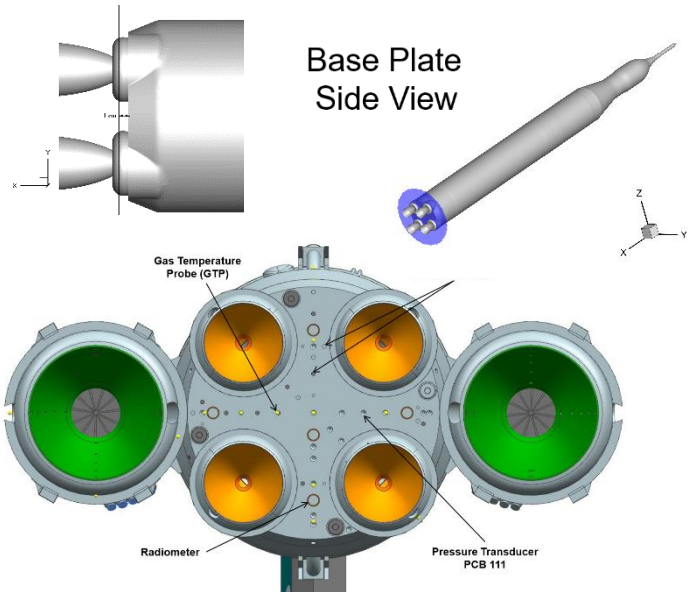

Figure 6. A schematic representation of the base plate showing the thin film, pressure and radiometer locations.

Optical fibers with a loss of less than 0.2 dB/m at the laser emission wavelength are used to bring the light into and out of the LENS II test section through vacuum-tight feedthroughs. Light from the laser source is coupled into a single-mode fiber using a numerical-aperture-matched reflective collimator from Thor Labs. An identical collimator but with a sapphire window to protect the optic is used to pitch the beam over the measurement path to a retro-reflecting mirror placed on the mass block that supports the model. After passing through the measurement region twice, the light is caught by a fiber-coupled reflective collimator matched to the numerical aperture of the multimode fiber used to pass the light out of the test section. A ZnSe asphere from Janos Technology, is used to focus the light from the end of the fiber onto a Kolmar KISDP-1-J1/DC InSb detector with a 15 MHz bandwidth. A high-speed acquisition system acquires approximately 170 ms of test data at 100 MHz. A narrow bandpass filter to eliminate the effect of light emission from the operation of the motors was initially also included in the optical setup but was later determined to be unnecessary.

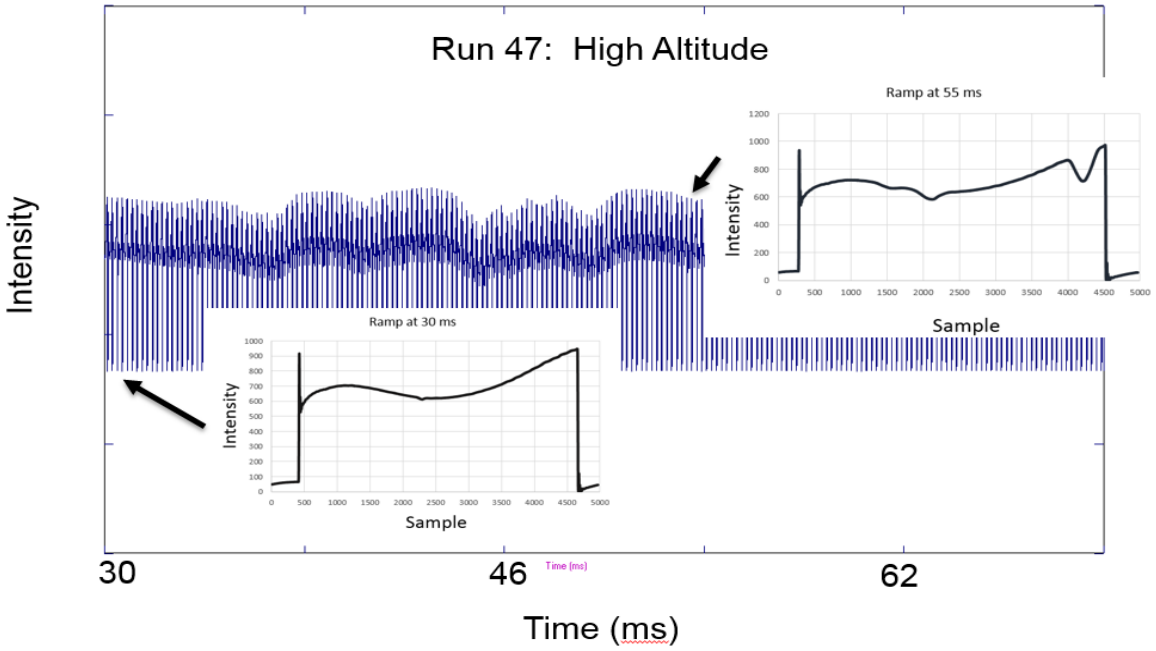

Figure 7. Aero-Optic effects on TDLAS measurement during a hot-fire test in LENS II.

Aero-optic effects can potentially affect the measurement by moving the beam around on the catch optic resulting in diminished or absent signal. This was a concern in particular since the total path length is relatively large and even small angle changes can result in substantial translation of beam spot and smearing of the beam in the plane of the catch optic. Early tests confirmed that for the M=0 cases (no tunnel flow), the aero-optic effects are not significant. Later tests with tunnel flow and at the prescribed altitudes, there was only bulk aero-optic effects which did little to modify the per-ramp measurement and analysis. As shown in Fig. 7, the 40 ms of TDLAS data or 200 ramps, captured during a hot-fire test did result in some intensity modulation of the beam, but this modulation was minor and of minimal impact for the 200 microseconds of a single scan. The single ramp traces pre-combustion are compared to a ramp captured during the middle of the run and is represented by the inset traces in Fig. 7.

The tunable diode laser absorption spectroscopy technique takes advantage of the fact that the current that is applied to the laser to cause it to emit, also heats the diode causing the laser cavity to change slightly. Besides increasing the number of photons that are emitted from the laser diode with increased current, the slight increase in temperature causes the wavelength of the emitted photons to vary slightly. A "saw tooth" current ramp that is applied to the diode results in a corresponding "saw tooth" intensity ramp observed by the detector. In addition as the bulk properties of the diode cavity changes with the ramp current the emitted photon wavelength increases linearly with the photon flux as well. For the current ramp applied to the diode in this work, a wavelength scan over approximately 0.415 nm was produced as represented by a single ramp in Fig. 7 and 8. The typical H_2O absorption feature is only about 0.02 nm in width for the pressure levels experienced during the ascension flight trajectory. For the full 0.415 nm laser wavelength scan there are six ro-vibrational transitions which have noticeable absorption strength. Some of the transitions have differing lower state energies. Because the relative population of these lower energy state levels

changes with temperature the measured absorption feature for these transitions will be observed to vary with temperature. A ratio of integrated strength of the absorption features will directly yield the temperature of the gas.

Rather than just compare the ratio of the integrated absorption features for two ro-vibrational levels within the selected scan interval of the laser, we sampled at 100 MHz or faster, and limited the scan frequency to less than 5 kHz so as not to smear the emission width of the laser during the scan. This preserved the precise line shape of the H_2O absorption features. With a high resolution line-by-line analysis the temperature, pressure and concentration were obtained from a fit of the 6 main absorption features within our chosen scan interval from 2713.8714 nm to 2714.2905 nm.

As shown in Fig. 8, while the photon flux increases with current, the wavelength of the emitted photons is increased as well. The wavelength increases from left to right on the graph. The red arrows denote transitions with higher lower state energy level values than the single transition marked by the blue arrow. That transition originates from a much lower energy level and it is therefore stronger at lower temperatures. At room temperature there is no significant absorption from the transitions marked with the red arrows.

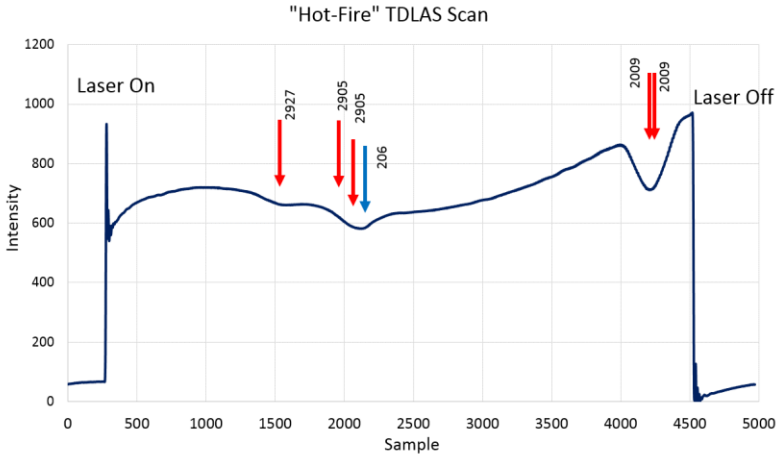

Figure 8. A single TDLAS scan is shown during a hot-fire test at high altitude. The six water absorption features are shown for the scan interval between 2713.8714 to 2714.2905 nm. The ro-vibrational transitions are designated along with their lower state energies.

B. Line-by-Line Model

The absorption of radiation due to molecular interaction with a photon beam has been described in detail in the literature. A summary of the relevant equations that are required for the line-by-line absorption model we have implemented to describe the TDLAS data follow.

The theory behind absorption spectroscopy is based on the Beer-Lambert law, which governs the absorption of monochromatic radiation through a uniform path length of a weakly absorbing medium.

$$\frac{I}{I_o} = exp(-k_\nu L) \tag{1}$$

The initial intensity of the beam as it leaves the source is described by I_o while the beam intensity after traversing a distance L is designated as I.

The spectral absorption coefficient is defined as,

$$k_\nu = S_i(T) P X_j \varphi_\nu \tag{2}$$

Where the linestrength data, $S_i(T)$ is obtained from the HITRAN 2008 database[12]. The spectral absorption coefficient contains the optical path length P, the molefraction of the absorbing species Xj and the line shape function φ_ν. For temperatures other than the reference temperature of 296 K, the partition function is used to solve for the temperature dependent linestrength,

$$S(T) = S(T_o)\frac{Q(T_o)}{Q(T)}\left(\frac{T_o}{T}\right) exp\left[\frac{hcE''}{k}\left(\frac{1}{T}-\frac{1}{T_o}\right)\right]\left[1-exp\left(\frac{-hc\nu}{kT}\right)\right]\left[1-exp\left(\frac{-hc\nu}{kT_o}\right)\right]^{-1} \tag{3}$$

Where the parameter $Q(T_o)$ is the partition function at the reference temperature T_o. The lineshape is a function of multiple types of broadening mechanisms the two dominating mechanisms in this study are Doppler broadening and

collisional broadening. Doppler broadening is caused by the random thermal motion of the absorbing molecules and follows a Maxwellian velocity distribution, resulting in a Gaussian lineshape.

$$\varphi_D(\nu) = \frac{2}{\Delta\nu_D}\left(\frac{ln(2)}{\pi}\right)^{1/2} exp\left[-4ln(2)\left(\frac{\nu-\nu_o}{\Delta\nu_D}\right)^2\right] \tag{4}$$

The Doppler full width at half maximum (FWHM) is given below, where the final expression is simplified from the intermediate expression to work in wavenumber units (cm^{-1}).

$$\Delta\nu_D = \nu_o\left[\frac{8kTln(2)}{mc^2}\right]^{1/2} = 7.1623x10^{-7}\left[\nu_o\left(\frac{T}{M}\right)^{1/2}\right] \tag{5}$$

Collisional broadening occurs when molecules collide with each other and is modeled using the Lorentzian function. It is assumed that the collisions are binary and that the transition time is fast compared to the collision duration, and is given by,

$$\varphi_C(\nu) = \frac{1}{\pi}\frac{\frac{\Delta\nu_C}{2}}{(\nu-\nu_o)^2+\left(\frac{\Delta\nu_C}{2}\right)^2} \tag{6}$$

The collisional FWHM is given by the expression,

$$\Delta\nu_C = 2P\left(\frac{T_o}{T}\right)^n\left[X\delta_{self} + (1-X)\delta_{air}\right] \tag{7}$$

The self-broadening half-width and air-broadening half-width are obtained from the HITRAN database. These values are listed in table 1, for the six transitions used in this work. Doppler broadening is dominant at lower pressure, while at higher pressures, collisional broadening is dominant. If the Doppler and collisional FWHM values are comparable, then a Voigt profile is needed, and describes the convolution of the two line shapes. A Voigt profile was used in this work however since most of the measurements were at very low pressure, representative of high altitudes, the dominant line shape was described by Doppler broadening due to the thermal motion of the molecules, assuming the gas is at rest relative to the probe beam.

A second mechanism that affects the measured line shape significantly especially at the higher altitudes, is the Doppler line shift which is due to the local velocity vector of the bulk gas relative to the optical path of the laser beam. This phenomena is frequently used at the LENS facilities to measure the free stream velocity of the test gas in the tunnel [(13)].

A laser source is projected at an angle ϕ relative to the flow velocity vector. During the wavelength scan, the emission wavelength of the photons from the QCL laser source are at slightly longer wavelengths as the intensity increases with supply current. Typically we place a return mirror on the opposite side of the flow, so that the beam path samples the absorbing molecules both coming and going at the angle ϕ. The basic Doppler shift equation is shown in Fig. 9, with a schematic representing the optical path of the probe beam relative to the bulk gas velocity of the freestream gas. The QCL laser scans from shorter wavelength at low applied current to longer wavelength as current/intensity is increased. From the probe molecule rest frame, the source photons with the flow appear to have a longer wavelength than the actual wavelength of the photon emitted in the laboratory frame. Thus the absorption feature will occur later in the scan time of the laser source in the lab frame. Likewise a second laser beam that is oriented against the flow will experience absorption earlier in the ramp cycle of the laser at shorter wavelength. The combined temporal

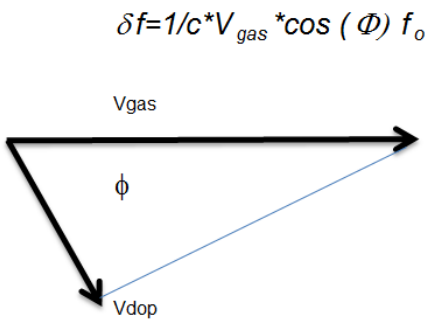

Figure 9. The Doppler shift phenomena is sensitive to the angle between the flow vector and the sensing beam vector.

shift between the two measured absorption features can then be reduced to velocity by application of the Doppler shift formula. The Doppler shift effect is greatest when the angle between the gas velocity vector and the laser beam is at zero degrees or 180 degrees. This was the case for the measurements reported here, as we shall see the Doppler shift significantly modifies the shape of the H_2O absorption features at the higher altitude conditions.

C. Computational Fluid Dynamics Code

Computational Fluid Dynamics (CFD) simulations were performed [14] for several altitudes for the Core-only configuration using the DPLR CFD code. In these cases, several simplifications were made – the vehicle is computed 1/8th by symmetry, smooth OML was considered, the core engine gas is assumed to be fully burned in the combustion

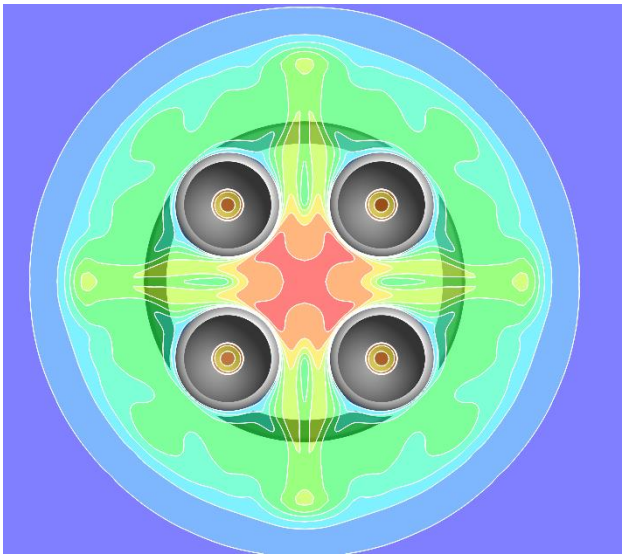

Temperature distribution at 150 kft

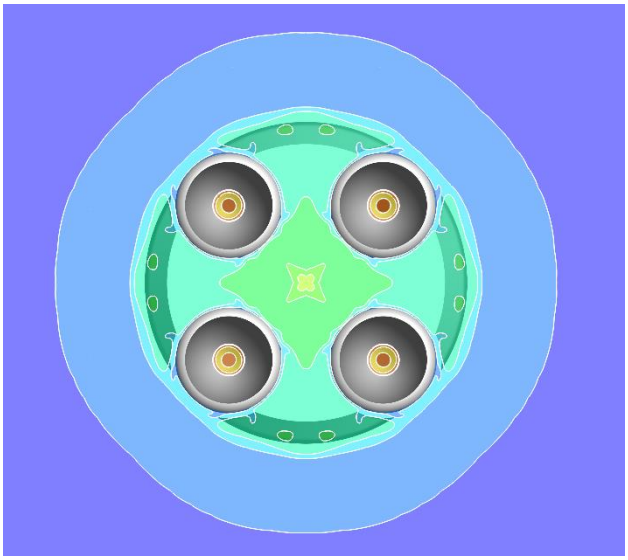

Temperature distribution at 100 kft

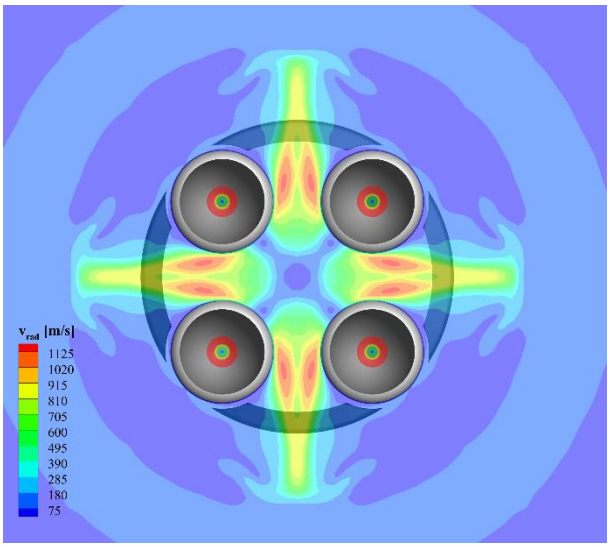

Velocity distribution at 150 kft

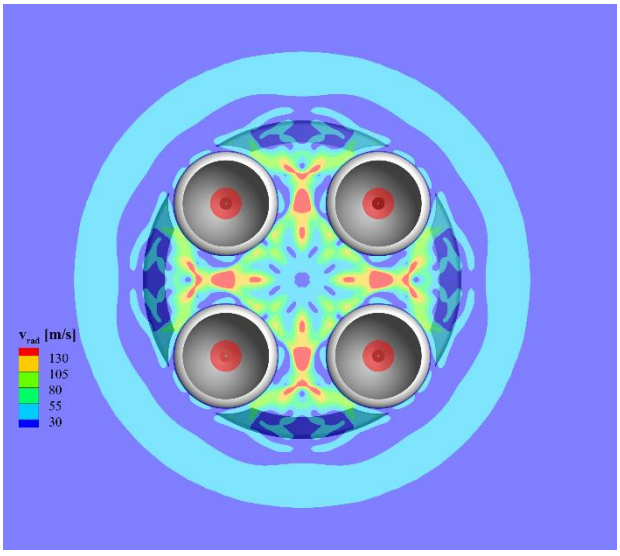

Velocity distribution at 100 kft

Figure 10. A CFD computation of the temperature distribution across the base plate at high altitude.

chamber such that the product gas composition is water (H_2O), and the freestream Air is assumed to be of inert composition. The simulations were composed of approximately $8x10^6$ structured grid cells and calculation convergence was monitored until the heat flux field over the base region stabilized and ceased to change significantly as the calculation was advanced in time. The diverging section of the nozzle interior is included in the simulation to approximate the boundary layer growth on the inner wall surface starting from just downstream of the throat. The resulting velocity, temperature, and water vapor composition along the base region within the line-of-sight of the TDLAS measurements is thus a direct function of the relative updraft strength that determines how dilute the exhaust plumes are and how much water vapor reaches the base region. In Fig. 10 the temperature and velocity profiles along the base region for a high altitude is shown on the left panel. The right panel shows the temperature and velocity profiles for a low altitude case. The CFD calculation indicates that there is significant radial velocity of the flow along the base region at high altitude. In the peak region the effect on the TDLAS measurement would be to cause separation of the Doppler shifted absorption feature, such that two peaks would be clearly distinguishable. Especially for the doublet at 3684.25 cm^{-1}, see Fig. 11. At the lower altitudes the radial velocity of the base flow gas is small and causes minor perturbation of the absorption feature.

III. Experimental Results and Discussion

A. Line-by-Line Spectra Simulation Code

A line-by-line calculation is used in this work to fit the TDLAS spectra obtained during hot-fire tests with the SLS model in a vacuum environment no flow, and at a given effective altitude with flow where Mach number and density are matched to a given point in the flight trajectory of the SLS vehicle. The diode laser is scanned over a very narrow spectral interval at 5 kHz such that the six absorption features due to H_2O are measured dynamically as the engines burn and produce a large amount of heated water as an exhaust by-product. The optical beam traverses the center of the base plate of the SLS model. The CFD results indicate that there are in general two zones, where the average temperature is roughly at different mean values. Rather than using a single zone calculation we have split the optical path into two regions, the central zone 1, and the outer ring zone 2. It is notable that both for the lower altitude case and the high altitude case the CFD indicates that there is significant hot H_2O extending considerably beyond the physical dimension of the base plate. Therefore in this work the central zone is set to 16 cm diameter while the outer zone is set to about 40 cm. Early analysis of the TDLAS data with the line-by-line model showed marked disagreement in feature absorption width for the high altitude cases. Examination of the CFD results for high altitude show that there is significant radial velocity at high altitude. The Doppler shift phenomena was then included in the line-by-line model and good fits to the data were obtained.

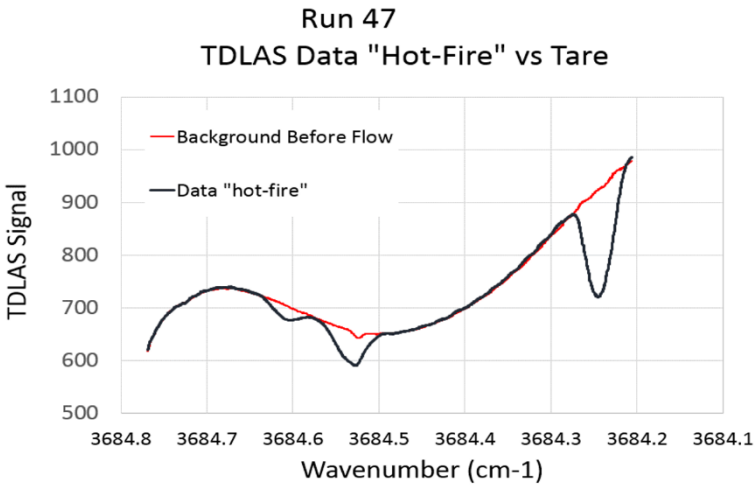

Figure 11. The pre-flow absorption or "Tare" trace provides the background level used in line-by-line calculations. The background trace is compared to a data trace during the hot-fire test.

The six primary H_2O lines that are included in the line-by-line model calculations are listed in table 1. The HITRAN 2008 data base was used as the primary reference for this work. In previous work the HITRAN data was checked against hot cell measurements of H_2O absorption at temperatures and pressures similar to the expected conditions for the hot fire experiment [15].

molecule	ν	$S_o(296)$	γ_{air}	γ_{self}	E"	n
	cm^{-1}	$cm^{-1}/(molecule\ atm^{-1})$	$cm^{-1}\ atm^{-1}$	$cm^{-1}\ atm^{-1}$	cm^{-1}	
11	3684.24	8.03E-23	0.0262	0.2249	2009.81	0.49
11	3684.25	2.68E-23	0.0234	0.2249	2009.81	0.49
11	3684.53	3.93E-21	0.094	0.585	206.301	0.77
11	3684.54	1.00E-24	0.0377	0.3841	2905.43	0.59
11	3684.54	3.32E-25	0.0374	0.3841	2905.43	0.59
11	3684.61	4.92E-25	0.0373	0.2143	2927.94	0.37

Table 1. HITRAN 2008 H_2O transitions

Many TDLAS ramps are measured before the tunnel flow arrives over the model. These tare data are used to describe the background absorption level used in the line-by-line model calculations. For example in Fig. 11, a single ramp before flow is plotted against the run data as previously shown in Fig. 7. The background signal has a sinusoid intensity variation which is primarily due to the small amount of H_2O vapor in the laboratory optical path external to the test section containing the hot-fire vehicle. The lab has about 0.01 percent H_2O by mole-fraction and because the pressure is 1 atmosphere, the collision line width is larger than the scan interval chosen for this experiment, thus resulting in the sinusoid absorption feature due to the blue transition shown in Fig. 8. The background absorption signal also shows a small amount of absorption at 3684.55 cm^{-1} which is due H_2O throughout the large optical path from the top of the tunnel where the launch and receive optics are located to the retroreflector mirror mounted to the floor and back again. Before the run the background pressure in the tunnel is less than 0.001 atm, the optical path is approximately 425 cm and the residual gas is at room temperature. The magnitude of the small absorption feature in Fig. 11 pre-run is consistent with the tunnel conditions.

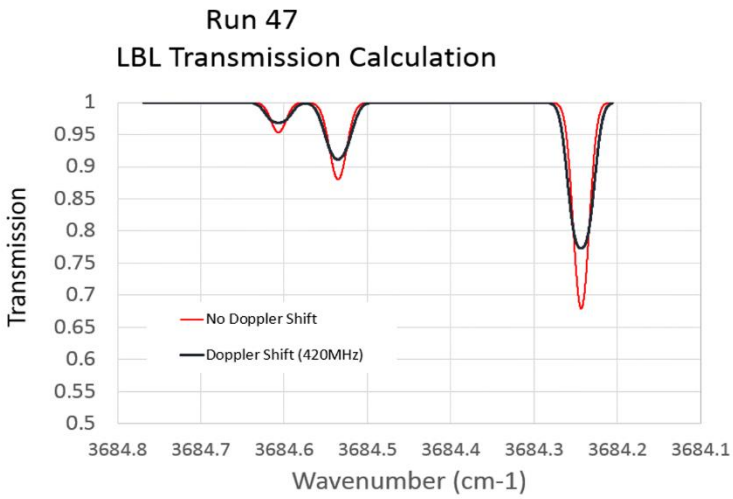

Figure 12. A two zone line-by-line transmission calculation for the six H_2O lines listed in table 1 is shown. Two calculations are shown where the effect of the bulk motion of the gas is to broaden the absorption features.

The background trace of Fig 11 is used as the baseline to a line-by-line calculation using the six ro-vibrational H_2O transitions listed in table 1. The calculation is split into two zones a central zone with an average temperature of about 52 arbitrary temperature units (atu), 16 cm in length with an average pressure of 0.0025 atm, followed by a second larger zone which extends beyond the physical base plate dimensions as indicated by our CFD calculations. The second zone has an average temperature of about 40 atu, 40 cm in length with an average pressure of 0.0013 atm. In addition the line-by-line transmission calculations were also performed assuming a Doppler line shift of 0.014 cm^{-1}. The results of the line-by-line calculations are shown in Fig 12. Clearly the Doppler shift contributes to increasing the absorption feature width. For high altitude measurements it is necessary to include the doppler shift. There is no temperature/pressure combination that will yield a broad enough absorption feature. For some high altitude runs the radial velocity of the gas is so high that one observes two clearly distinguishable peaks for the feature located at 3684.25 cm^{-1}.

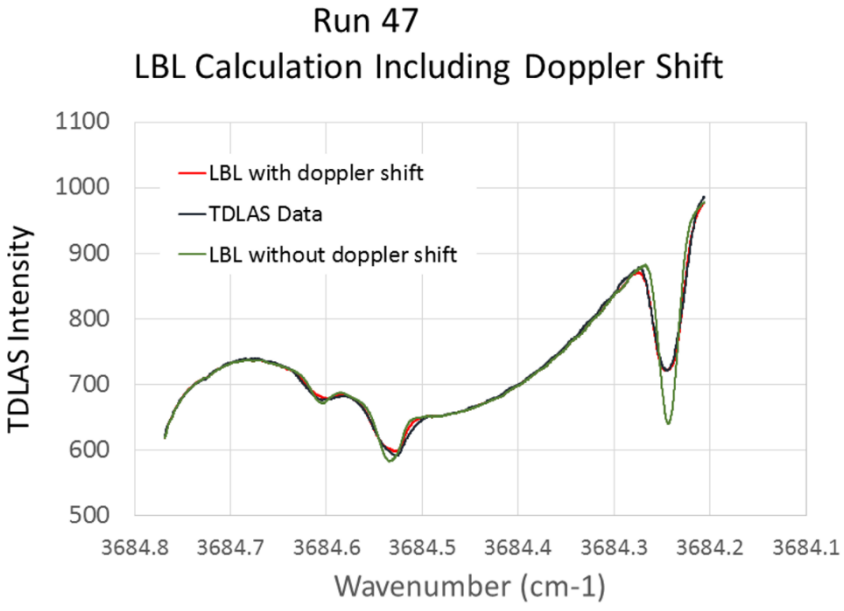

Figure 13. The hot-fire absorption signal is compared to a tare plus line-by-line calculation, with and without the Doppler shift effect.

In an effort to extract the average gas temperature along the base plate, the background trace from Fig. 11 is multiplied by the transmission calculation Fig. 12 and compared to the measured TDLAS data. This is shown in Fig 13 where the data and the two LBL calculations are compared. Obviously the doppler shift due to the bulk motion of the hot H_2O molecules is significant and must be included in the modeling. The required pressure levels and molefraction values for the two zones is consistant with guidance from CFD calculations and pressure measurements made on the base plate.

B. Temperature of heated H_2O gas above the base plate versus altitude.

The TDLAS technique was used to measure the combustion product gas temperature above the base plate for a 2 percent hot-fire model during tunnel runs simulating flow at Mach numbers and densities along the flight path of the vehicle as it transitions to space. Additional runs were performed at high altitude with no tunnel flow. The interaction between the nozzle exhaust for the four core engines and tunnel flow and sometimes including the Solid Rocket Boosters was investigated at a number of different altitudes and Mach numbers. There were 76 runs performed where the TDLAS instrument was on-line for the majority of cases. Many of the measurements were nominally repeats where modifications to the model or engines were performed, but where the gas temperature across the base plate should remain the same.

Each of these runs was analyzed according to the line-by-line technique discussed in the previous section. At the time of this writing single scans are analyzed for each test. However, the run time of the LENS II facility and the engine on time approach 50 milliseconds of steady flow. With a scan rate of the TDLAS instrument of 5 kHz there are about 200 ramps per run which need to be analyzed. A non-linear least squares technique is being implement with the line-by-line modeling effort described here to automate the data reduction process. However, it should be noted that the fluctuation of the absorption traces during a run is minor and the propitious choice of one or two good representative ramps per run is expected to yield the average gas temperature to within a few hundreds of degrees kelvin. In Fig. 14 the normalized average gas temperature above the base plate is plotted as a function of altitude. The individual runs represent cases where the engines were fired with different chamber pressure, nozzle gimbal angle etc. One should use caution making any assumptions from this plot. More detailed run by run information is available. The two sets of data represent the average temperature in central zone compared to the outer zone as described above. When compared against CFD it appears that the hot central zone is at least 30 % higher in temperature than the outer zone. For the highest altitude case the central zone temperature appears to be double the outer zone temperature. This corresponds to our CFD calculations. Fig. 14 shows that the temperature measurements begin to deviate significantly from a linear trend line at higher altitudes. From table 1 it is clear that five of the transitions used in this work have very nearly the same lower state energy, about 2900 cm-1. Therefore there is little sensitivity in the change of the magnitude of the integrated absorption features as a function of temperature. The line-by-line calculation is then most sensitive to shape effects of the absorption features as temperature increases. It would be more desirable to have a line or two with a lower state energy about half of the five high temperature lines in this work. The lower temperature measurements at low altitude are very sensitive since besides the five hot lines, there is

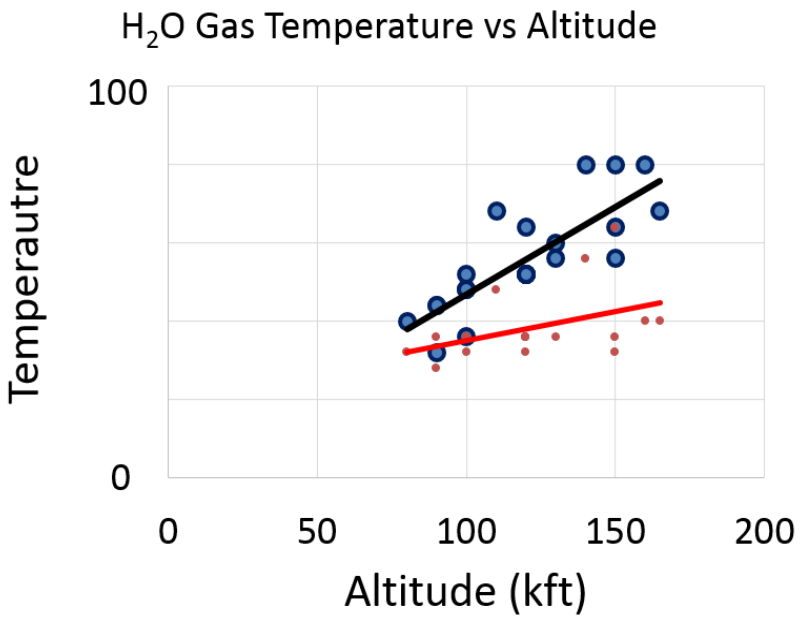

Figure 14. The gas temperature above the base plate as a function of altitude. Zone 1 is centered on the base plate. Zone 2 is at lower temperature.

a single low temperature line at 3684.55 cm-1. The line-by-line fit in these cases is dominated by the relative change in the magnitude of this low temperature line compared to the five high temperature lines. In addition, from ramp to ramp the absorption curve is affected by subtle line shape fluctuations which are due to changes in the refractive environment, but also rapid changes in the local radial velocity of the gas over the base plate. Therefore a better average measurement of the temperature must include analysis of multiple sampling of the hot flow during the entire 40 milliseconds of combustor burn time.

IV. Conclusions

A high resolution tunable diode laser spectrometer has been installed in the LENS II shock tunnel at CUBRC to study the effect of nozzle exhaust plume interaction with the flow and subsequent effects on the heating rate of the base plate for a 2%-scale hot-fire model as part of NASA's development of the SLS vehicle. The TDLAS spectrometer was built to measure the temperature of the heated H_2O molecules which are combustion products of the H_2/O_2 core engines and the solid rocket motors. The gas temperature was measured as a function of altitude with and without tunnel flow for various conditions which represent the highest heating rates during SLS ascent into space. The spectrometer provided good average temperature information and in addition provided the radial velocity of the gas flowing over the base plate for high altitude. Improvements to the technique were identified, these include selecting a better choice of scan range where a number of water transitions are sampled with varying lower state energies to improve the temperature sensitivity especially at high temperature. In addition an automated least-square line-by-line code is being built to analyze the more than 10,000 individual ramp measurements that are represented by this work, and future work.

Acknowledgments

This work was sponsored by the NASA contract…..

References

1. Fuller, C E, et al., et al. *Utilization of a Gas Temperature Recover Probe on Space Shuttle Short Duration Base Heating Model Tests OH-78 and IH-39.* 1977. RTR-019-2, Remtech Inc..
2. Fuller, C E, Powell, R T and Levie III, J K. *Diagnostic Evaluation Testing of a Gas Recover Temperature Probe in the NASA/MSFC Impulse Base Flow Facility.* 1978. NASA-CR-161500, Remtech Inc..
3. East, R A and Perry, J H. *A Short Time response Stagnation Temperature Probe.* Aeronautical Research Council. 1967. CP No. 909.
4. *High Bandwodth Stagnation Temperature Measurements in a Mach 6 Gun Tunnel Flow.* Buttsowrth, D R and Jones, T V. 2, 2003, Experimental Thermal and Fluid Science, Vol. 27, pp. 177-186.
5. *Space Launch System Base Heating Test: Sub-Scale rocket Engine/Motor Design.* Mehta, M, et al., et al. Washington D.C. : AIAA 2014-1255, 2014. 52nd Aerospace Sciences Meeting.
6. *Sub-Scale Space Launch System Core-Stage Rocket Engine Development for Short-Duration Testing.* Mehta, M, et al., et al. Albuquerque, New Mexico : JANNAF Paper no. 3575, 8-11 December 2014. 46th Combustion / 34th Airbreathing Propulsion / 34th Exhaust Plume and Signatures / 28th Propulsion Systems Hazards Joint Subcommittee Meeting.
7. *Sub-Scale Space Launch System Solid Rocket Booster Development for Short-Duration Testing.* Mehta, M A, et al., et al. Albuquerque, NM : JANNAF Paper no. 3576, 8-11 December 2014. 46th Combustion / 34th Airbreathing Propulsion / 34th Exhaust Plume and Signatures / 28th Propulsion Systems Hazards Joint Subcommittee Meeting.
8. *High-Resolution Spectroscopy of Combustion Gases Using a Tunable Diode IR Laser.* Hanson, R K, Kuntz, P A and Kruger, C H. 8, 1977, Applied Optics, Vol. 16, pp. 2045-2048.
9. Struve, Walter S. *Fundamentals of Molecular Spectroscopy.* New York : John Wiley & Sons, 1989.

10. Demtroder, W. *Laser Spectroscopy Basic Concepts and Instrumentation.* Berlin : Springer-Verlag, 1988.
11. Nanoplus. Single mode distributed feedback (DFB) lasers in near and mid infrared region. *Nanoplus website.* [Online] Nanoplus. http://nanoplus.de/index.php?option=com_content&view=article&id=23&Itemid=61.
12. *The HITRAN 2008 Molecular Spectroscopic Database.* Rothman, L S, et al., et al. 2009, Journal of Quantitative Spectroscopy & Radiative Transfer, Vol. 10, pp. 53-572.
13. Parker, R.; Wakeman, T; MacLean. M.; and Holden, M. "Measuring Nitric Oxide Freestream Velocity Using Quantum Cascade Lasers at CUBRC". AIAA Paper 2007–1329. 45TH Aerospace Sciences Meeting & Exhibit. Reno, NV: 8-11 January 2007.
14. Dufrene, A. et al., "Space Launch System (SLS) Base Heating Test: Experimental Operations and Results," 54th AIAA Aerospace Sciences Meeting, San Diego, CA, 2016.
15. Carr, Z., Parker, R., Dufrene, A., and Mehta, M. (2014), "Development of a TDLAS Instrument for Plume and Base Temperature Measurements of Sub-Scale Hot-Fire Rockets", JANNAF Paper No. 3736, 46th Combustion / 34th Airbreathing Propulsion / 34th Exhaust Plume and Signatures / 28th Propulsion Systems Hazards Joint Subcommittee Meeting, 8 – 11 December 2014, Hyatt Regency Albuquerque, Albuquerque, New Mexico.